Revised Version of PF#POF20-AR-01343

Rivulet Flow Down a Slippery Substrate

Abdulwahed S. Alshaikhi,[1,*] Stephen K. Wilson,[1,†] and Brian R. Duffy[1,‡]

[1] *Department of Mathematics and Statistics, University of Strathclyde, Livingstone Tower, 26 Richmond Street, Glasgow G1 1XH, UK*

(Dated: 12th May 2020, revised 26th June 2020)

A detailed analysis of small-scale locally unidirectional gravity-driven rivulet flow with prescribed volume flux down an inclined slippery substrate for a rivulet with either constant width (*i.e.*, pinned contact lines) or constant contact angle is undertaken. In particular, we determine the effect that varying the Navier slip length λ (*i.e.*, the strength of the slip at the solid–fluid interface) has on the rivulet. The present analysis shows that the shape and size of the rivulet and the velocity within it depend strongly on the value of λ. Increasing the value of λ reduces the viscous resistance at the substrate and hence leads to a larger velocity within the rivulet, and so the prescribed flux is achieved with a smaller rivulet. In particular, in the limit of strong slip, $\lambda \to \infty$, for a rivulet of a perfectly wetting fluid and a rivulet with constant width the velocity becomes large and plug-like like $O(\lambda^{1/2}) \gg 1$ and the rivulet becomes shallow like $O(\lambda^{-1/2}) \ll 1$, while for a rivulet with positive constant contact angle the velocity becomes large and plug-like like $O(\lambda^{2/3}) \gg 1$ and the rivulet becomes narrow like $O(\lambda^{-1/3}) \ll 1$ and shallow like $O(\lambda^{-1/3}) \ll 1$.

* abdulwahed.alshaikhi@strath.ac.uk

† Author for correspondence; s.k.wilson@strath.ac.uk

‡ b.r.duffy@strath.ac.uk

I. INTRODUCTION

Rivulet flows occur in a wide variety of physical contexts and over a wide range of length scales from nano and microfluidics to geophysical scales (see, for example, Darhuber and Troian [1] and Griffiths [2]). In many of these situations the appropriate boundary condition at the solid–fluid interface is the classical no-slip boundary condition, and, as a consequence of this, all of the previous theoretical work on rivulet flow of which the authors are aware has adopted this condition without comment. In the absence of a recent review of rivulet flow, see, for example, the recent papers by Alekseenko *et al.* [3], Herrada *et al.* [4], Mahady, Afkhami and Kondic [5], Howell *et al.* [6], and Al Mukahal, Duffy and Wilson [7, 8], and the references therein, for a representative selection of these previous studies. However, there are also many other situations in which for one reason or another the substrate is to some extent slippery and so the no-slip condition is not appropriate (see, for example, the review articles by Lauga, Brenner and Stone [9], Rauscher and Dietrich [10], Rothstein [11], Sochi [12], and Lee, Charrault and Neto [13]). Specifically, as Lauga *et al.* [9] stated, "the small-scale interactions between a liquid and a solid leads to extremely rich possibilities for slip behavior, with dependence on factors such as wetting conditions, shear rate, pressure, surface charge, surface roughness and dissolved gas". Furthermore, both Lauga *et al.* [9, Tables 19.1–19.4] and Nicholson *et al.* [14, Table 2] give summaries of experimental studies for a variety of combinations of fluid and substrate reporting a wide range of experimentally measured slip lengths ranging from zero (*i.e.*, no slip) to tens of micrometres, and (as, for example, Rothstein [11] describes) even larger slip lengths can be achieved by using superhydrophobic substrates. In particular, it is well established that a slip boundary condition is often appropriate to describe the behaviour of a fluid at the surface of a porous medium (see, for example, Beavers and Joseph [15], Jäger and Mikelić [16], Le Bars and Worster [17], and Nield [18]) and at a superhydrophobic textured surface impregnated with either gas or a lubricant (see, for example, Crowdy [19, 20], Schnitzer and Yariv [21], Alinovi and Bottaro [22], and Asmolov, Nizkaya and Vinogradova [23]). Motivated by our interest in these situations, and by the renewed interest in small-scale rivulet flows in the context of so-called "microfluidics with fluid walls" arising from the recent work by Walsh *et al.* [24], in the present work we undertake a detailed analysis of small-scale locally unidirectional gravity-driven rivulet flow with prescribed volume flux down an inclined slippery substrate for a rivulet with either constant width (*i.e.*, pinned contact lines) or constant contact angle. In particular, we determine the effect that varying the strength of the slip at the solid–fluid interface has on the rivulet.

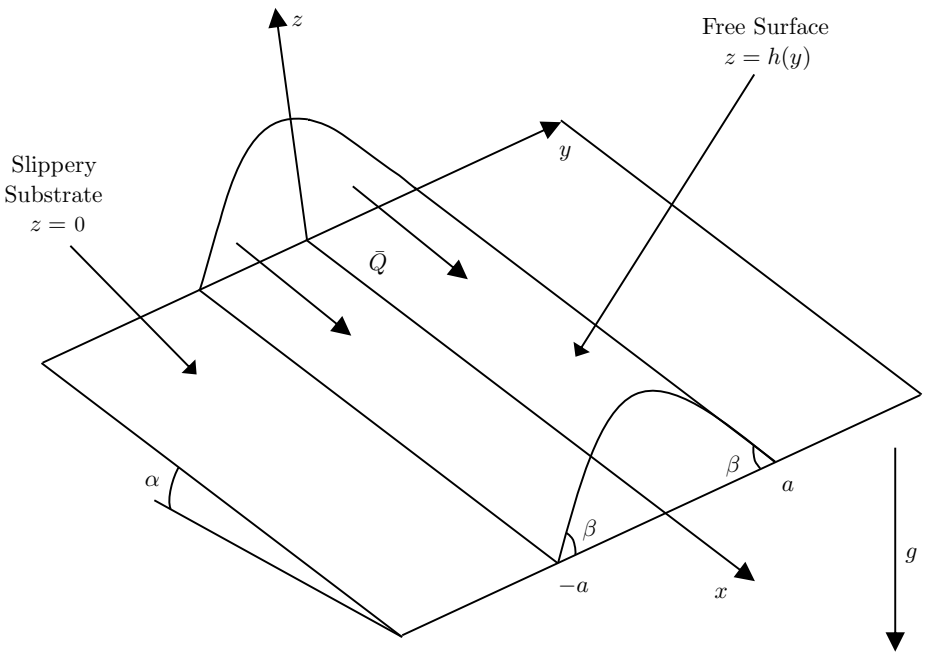

FIG. 1: Unidirectional gravity-driven flow of a thin symmetric rivulet with semi-width $a\,(>0)$, contact angle $\beta\,(\geq 0)$ and volume flux $Q\,(>0)$ down a slippery planar substrate inclined at an angle α $(0 \leq \alpha \leq \pi)$ to the horizontal.

II. PROBLEM FORMULATION

Consider the steady unidirectional gravity-driven flow of a thin symmetric rivulet with semi-width $a\,(>0)$, contact angle $\beta\,(\geq 0)$ and volume flux $Q\,(>0)$ of an incompressible Newtonian fluid with constant density ρ, viscosity μ and surface tension γ down a slippery planar substrate inclined at an angle α $(0 \leq \alpha \leq \pi)$ to the horizontal. To describe this situation we use Cartesian coordinates $Oxyz$ with the x-axis down the line of greatest slope, the y-axis horizontal, and the z-axis normal to the substrate $z = 0$. A sketch of the geometry of the problem is shown in Figure 1. The velocity $\mathbf{u} = u(y,z)\mathbf{i}$ and the pressure (relative to the constant atmospheric pressure) $p = p(y,z)$ satisfy the usual mass-conservation and Navier–Stokes equations. On the free surface, denoted by $z = h(y)$, the familiar normal and tangential stress conditions and the kinematic conditions hold, while at the contact lines $y = \pm a$ the thickness of the rivulet is, by definition, zero, *i.e.*, $h(\pm a) = 0$, and the contact angle is given by $\beta = \mp h'(\pm a)$, where the dash denotes differentiation with respect to argument. In contrast to previous studies, on the substrate $z = 0$ the usual no-slip condition $u(y,0) = 0$ is replaced by the simplest and most widely used slip condition, namely the Navier slip

condition (see, for example, Hocking [25])

$$u = \lambda \frac{\partial u}{\partial z} \quad \text{on} \quad z = 0, \tag{1}$$

where $\lambda\,(\geq 0)$ is the constant slip length. The maximum thickness of the rivulet (which, as we shall see, always occurs at $y = 0$) is denoted by $h_{\rm m} = h(0)$.

We non-dimensionalise the variables in the natural way by scaling y and a with ℓ, β with δ, z, h, $h_{\rm m}$ and λ with $\delta\ell$, u with $U = \delta^2\rho g\ell^2/\mu$, Q with $\delta\ell^2 U = \delta^3\rho g\ell^4/\mu$, and p with $\delta\rho g\ell$, where g is the magnitude of acceleration due to gravity, $\ell = (\gamma/\rho g)^{1/2}$ is the capillary length, and $\delta \ll 1$ is an appropriately defined transverse aspect ratio (see, for example, Paterson *et al.* [26, Sec. 2]). Henceforth all quantities are dimensionless unless stated otherwise.

At leading order in the limit of a thin rivulet, $\delta \to 0$, the velocity is given by

$$u = \frac{\sin\alpha}{2}\left[2h(z+\lambda) - z^2\right], \tag{2}$$

so that the slip velocity at the substrate is given by $u(y,0) = \sin\alpha\,\lambda h$ and the velocity of the free surface is given by $u(y,h) = \sin\alpha\, h(h+2\lambda)/2$, the local flux (*i.e.*, the depth integrated velocity), denoted by $\bar{u} = \bar{u}(y)$, is given by

$$\bar{u} = \int_0^h u(y,z)\,{\rm d}z = \frac{\sin\alpha}{3}h^2(h+3\lambda), \tag{3}$$

and the volume flux is given by

$$Q = \int_{-a}^{+a}\int_0^h u(y,z)\,{\rm d}z{\rm d}y = \int_{-a}^{+a}\bar{u}(y)\,{\rm d}y = \frac{\sin\alpha}{3}\int_{-a}^{+a} h^2(h+3\lambda)\,{\rm d}y. \tag{4}$$

The pressure is given by $p = \cos\alpha(h-z) - h''$, and the free surface shape satisfies

$$(h'' - \cos\alpha h)' = 0 \quad \text{subject to} \quad h(\pm a) = 0 \quad \text{and} \quad \beta = \mp h'(\pm a). \tag{5}$$

A. A Perfectly Wetting Fluid $\beta = 0$

In the special case of a perfectly wetting fluid with zero contact angle, $\beta = 0$, solving (5) shows that there is no rivulet solution for $0 \leq \alpha \leq \pi/2$, but there is a rivulet solution for $\pi/2 < \alpha \leq \pi$ given by

$$a = \frac{\pi}{m}, \quad h = \frac{h_{\rm m}}{2}(1+\cos my), \quad Q = \frac{\pi\sin\alpha}{24m}h_{\rm m}^2(5h_{\rm m}+18\lambda), \tag{6}$$

where we have introduced the convenient notation $m = |\cos\alpha|^{1/2}$.

B. A Non-Perfectly Wetting Fluid $\beta > 0$

In the general case of a non-perfectly wetting fluid with positive contact angle, $\beta > 0$, solving (5) shows that there is a rivulet solution given by

$$h = \frac{\beta}{m} H(ma, my), \quad h_{\rm m} = \frac{\beta}{m} H(ma, 0), \quad Q = \frac{\beta^3 \sin\alpha}{9m^4} f(ma) + \frac{\lambda \beta^2 \sin\alpha}{m^3} g(ma), \tag{7}$$

where the function $H = H(ma, my)$ is given by

$$H = \begin{cases} \dfrac{\cosh ma - \cosh my}{\sinh ma} & \text{for} \quad 0 \le \alpha < \dfrac{\pi}{2}, \\ \dfrac{(ma)^2 - (my)^2}{2ma} & \text{for} \quad \alpha = \dfrac{\pi}{2}, \\ \dfrac{\cos my - \cos ma}{\sin ma} & \text{for} \quad \dfrac{\pi}{2} < \alpha \le \pi, \end{cases} \tag{8}$$

the function $f(ma)$ is given by

$$f(ma) = \begin{cases} 15ma \coth^3 ma - 15 \coth^2 ma - 9ma \coth ma + 4 & \text{for} \quad 0 \le \alpha < \dfrac{\pi}{2}, \\ \dfrac{12}{35}(ma)^4 & \text{for} \quad \alpha = \dfrac{\pi}{2}, \\ -15ma \cot^3 ma + 15 \cot^2 ma - 9ma \cot ma + 4 & \text{for} \quad \dfrac{\pi}{2} < \alpha \le \pi, \end{cases} \tag{9}$$

and the function $g(ma)$ is given by

$$g(ma) = \begin{cases} 3ma \coth^2 ma - 3 \coth ma - ma & \text{for} \quad 0 \le \alpha < \dfrac{\pi}{2}, \\ \dfrac{4}{15}(ma)^3 & \text{for} \quad \alpha = \dfrac{\pi}{2}, \\ 3ma \cot^2 ma - 3 \cot ma + ma & \text{for} \quad \dfrac{\pi}{2} < \alpha \le \pi. \end{cases} \tag{10}$$

Note that the function $f(ma)$ was first obtained by Duffy and Moffatt [27] in their pioneering study of the case $\lambda = 0$, while the function $g(ma)$ was first obtained by Sullivan *et al.* [28] in their study of rivulet flow in the presence of a uniform longitudinal surface shear stress τ. There is, in fact, a close relationship between the present problem and the corresponding problem of a rivulet in the presence of a uniform longitudinal surface shear stress studied by Wilson and Duffy [29], Sullivan *et al.* [28], Wilson, Sullivan and Duffy [30], and Paterson *et al.* [31]. Specifically, while the velocity for the shear-stress problem given by

$$u = \frac{\sin\alpha}{2}(2h - z)z + \tau z \tag{11}$$

is qualitatively different from that for the present problem given by (2), the corresponding expressions for both $\bar{u}$ and Q coincide exactly if we replace τ with $2\lambda \sin\alpha$. Figure 2 confirms that, even with this special choice of τ, and for the

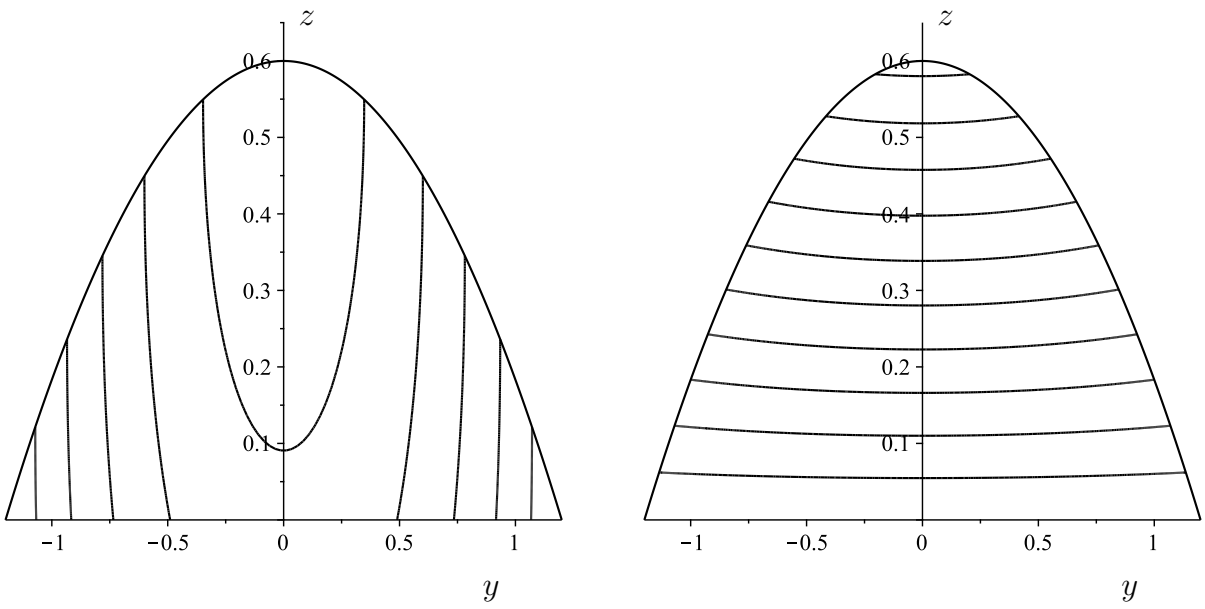

FIG. 2: Contour plots of the velocity $u(y,z)$ given by (a) equation (2) for the present problem with $\lambda = 2$ and by (b) equation (11) for the corresponding problem of a rivulet in the presence of a uniform longitudinal surface shear stress with $\tau = 2\lambda \sin\alpha = 4$. In both cases $\alpha = \pi/2$, $a \simeq 1.1998$, $\beta = 1$ and $Q = 1$. The contour interval is 0.25 in both (a) and (b).

same values of α, a, β and Q, the velocity profiles given by (2) for the present problem with $\lambda = 2$ and by (11) for the corresponding shear-stress problem with $\tau = 2\lambda \sin\alpha = 4$ are qualitatively different. Note, however, that whereas in the shear-stress problem the shear stress τ can take any value (positive, negative or zero), in the present problem the slip length λ cannot be negative, and so solutions of the shear-stress problem with $\tau < 0$ have no equivalent in the present problem. Moreover, note that the previous work on the shear-stress problem with a constant value of τ corresponds to the physically implausible situation in which λ depends on α like $1/\sin\alpha$. In light of the previous work on the shear-stress problem, in the present work we focus on the novel features of the present problem, namely the dependence of the rivulet on the values of α, λ and Q.

Figure 3 illustrates the effect of varying λ on the velocity profile given by (2). For small values of λ (such as that shown in Figure 3(a)) the velocity approaches the familiar semi-parabolic in z profile in the case $\lambda = 0$, namely $u \sim \sin\alpha\,(2h - z)z/2$, whereas for large values of λ (such as that shown in Figure 3(b)) the velocity profile becomes plug-like in z (*i.e.*, independent of z but not y), namely $u \sim \sin\alpha\,\lambda h$, and so the contours become straight lines perpendicular to the substrate.

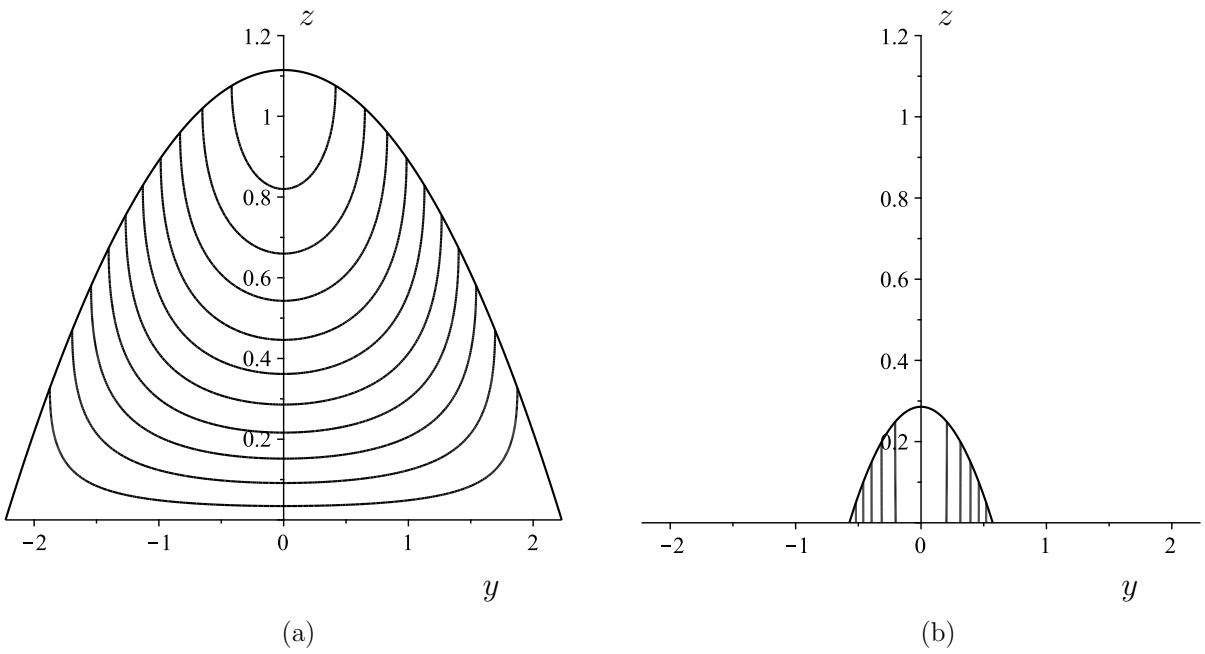

FIG. 3: Contour plots of the velocity $u(y,z)$ given by (2) when (a) $\lambda = 0.02$ and $a \simeq 2.2293$ and (b) $\lambda = 20$ and $a \simeq 0.5716$. In both cases $\alpha = \pi/2$, $\beta = 1$ and $Q = 1$. The contour interval is 0.06 in (a) and 1 in (b).

C. Locally Unidirectional Flow Down a Slowly Varying Substrate

The solutions for unidirectional flow of a uniform rivulet presented in subsections II A and II B for perfectly wetting and non-perfectly wetting fluids, respectively, relate the angle of inclination α, the semi-width a, the contact angle β, the maximum thickness $h_{\rm m}$, and the flux Q of the rivulet, and may be interpreted in a variety of ways. In what follows we follow, for example, Duffy and Moffatt [27] and Paterson *et al.* [26], and use these solutions to describe the locally unidirectional flow of a slowly varying rivulet with prescribed constant flux $Q = \bar{Q}\,(> 0)$ together with either prescribed constant semi-width $a = \bar{a}\,(> 0)$ (*i.e.*, pinned contact lines) and slowly varying contact angle $\beta\,(\geq 0)$ or prescribed constant contact angle $\beta = \bar{\beta}\,(\geq 0)$ and slowly varying semi-width $a\,(> 0)$ down a slowly varying substrate. Specifically, for definiteness, we consider rivulet flow in the azimuthal direction from the top, corresponding to $\alpha = 0$, to the bottom, corresponding to $\alpha = \pi$, of a large horizontal cylinder (although other interpretations are, of course, also possible).

III. A RIVULET OF A PERFECTLY WETTING FLUID $\beta = \bar{\beta} = 0$

Setting $Q = \bar{Q}$ in (6) yields a cubic polynomial equation for h_{m}, namely

$$h_{\mathrm{m}}^3 + \frac{18\lambda}{5} h_{\mathrm{m}}^2 - \frac{24\bar{Q}m}{5\pi \sin\alpha} = 0. \tag{12}$$

In the special case $\lambda = 0$ we recover the solution for $h_{\mathrm{m}} = h_{\mathrm{m}0}$ first obtained by Wilson and Duffy [29], namely

$$h_{\mathrm{m}0} = \left(\frac{24\bar{Q}m}{5\pi \sin\alpha} \right)^{\frac{1}{3}}, \tag{13}$$

while in the general case $\lambda > 0$ the solution for h_{m} is

$$h_{\mathrm{m}} = \frac{6\lambda}{5} \left\{ 2\cos\left[\frac{1}{3} \cos^{-1}\left(\frac{25\bar{Q}m}{18\pi\lambda^3 \sin\alpha} - 1 \right) \right] - 1 \right\} \tag{14}$$

when $0 < 25\bar{Q}m \leq 36\pi\lambda^3 \sin\alpha$ and

$$h_{\mathrm{m}} = \frac{6\lambda}{5} \left\{ 2\cosh\left[\frac{1}{3} \cosh^{-1}\left(\frac{25\bar{Q}m}{18\pi\lambda^3 \sin\alpha} - 1 \right) \right] - 1 \right\} \tag{15}$$

when $25\bar{Q}m \geq 36\pi\lambda^3 \sin\alpha$. Note that replacing λ with $\tau/(2\sin\alpha)$ in (14) and (15) recovers the corresponding solutions obtained by Sullivan *et al.* [28] (their equations (A.2) and (A.5) with (A.6) and (A.7)) for the shear-stress problem in the case $\tau > 0$.

Figures 4 and 5 show plots of the semi-width $a = \pi/m$ (which is independent of both λ and $\bar{Q}$) and the maximum thickness h_{m} given (13)–(15) as functions of the scaled angle α/π for a range of values of λ and $\bar{Q}$, respectively. In particular, Figures 4 and 5 illustrate that a is a monotonically decreasing function of α and h_{m} is a monotonically increasing function of α, and that for $\lambda > 0$ the rivulet becomes wide and shallow according to

$$a \sim \pi \left(\alpha - \frac{\pi}{2} \right)^{-\frac{1}{2}} \to \infty \quad \text{and} \quad h_{\mathrm{m}} \sim \left(\frac{4\bar{Q}}{3\pi\lambda} \right)^{\frac{1}{2}} \left(\alpha - \frac{\pi}{2} \right)^{\frac{1}{4}} \to 0^+ \tag{16}$$

as $\alpha \to \pi/2^+$, and deep with finite semi-width $a = \pi$ according to

$$a = \pi + \frac{\pi}{4}(\pi - \alpha)^2 + O\left((\pi - \alpha)^4 \right) \to \pi^+ \tag{17}$$

and

$$h_{\mathrm{m}} = \left(\frac{24\bar{Q}}{5\pi(\pi - \alpha)} \right)^{\frac{1}{3}} - \frac{6\lambda}{5} + O\left((\pi - \alpha)^{\frac{1}{3}} \right) \to \infty \tag{18}$$

as $\alpha \to \pi^-$. Figure 4 also illustrates that h_{m} is a monotonically decreasing function of λ, and that the rivulet approaches its finite maximum thickness in the case $\lambda = 0$ given by (13) from below according to

$$h_{\mathrm{m}} = \left(\frac{24\bar{Q}m}{5\pi \sin\alpha} \right)^{\frac{1}{3}} - \frac{6}{5}\lambda + O\left(\lambda^2 \right) \to h_{\mathrm{m}0}^- \tag{19}$$

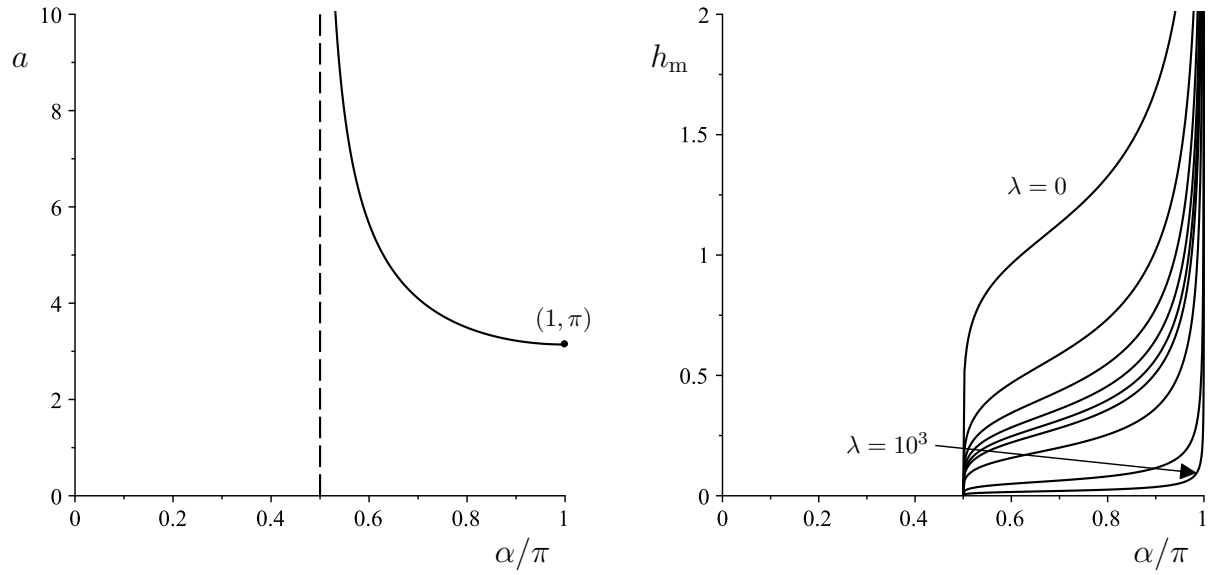

(a) (b)

FIG. 4: Plots of (a) the semi-width $a = \pi/m$ (which is independent of λ) and (b) the maximum thickness $h_{\rm m}$ given by (13)–(15) as functions of the scaled angle α/π for a rivulet of a perfectly wetting fluid with $\beta = \bar{\beta} = 0$ for $\lambda = 0, 1, 2, 3, 4, 5, 10, 10^2, 10^3$ when $\bar{Q} = 1$.

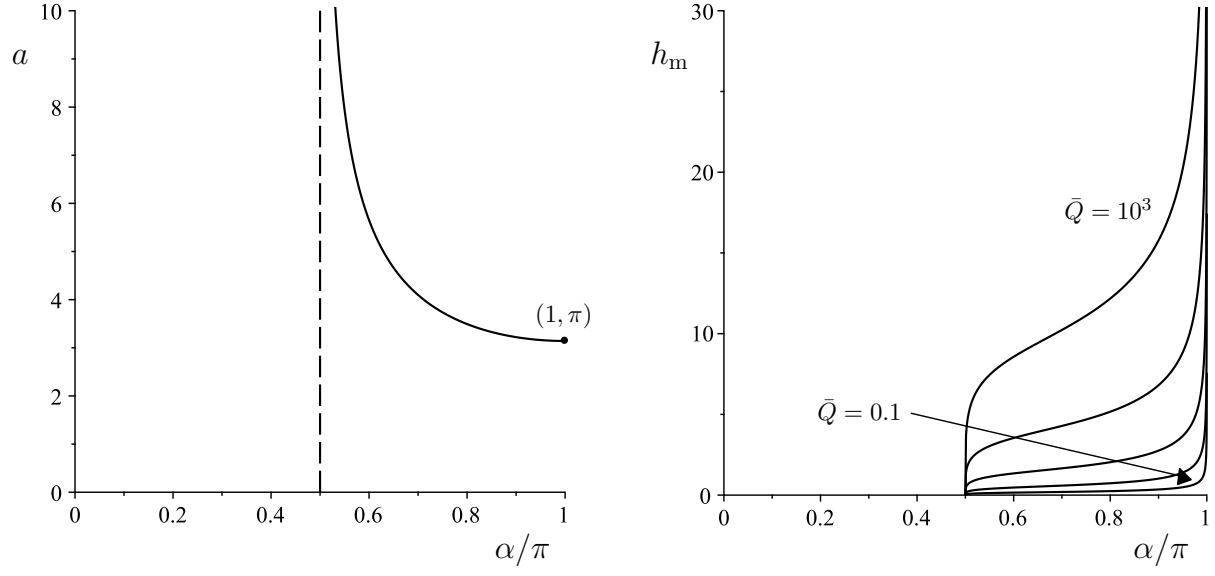

(a) (b)

FIG. 5: Plots of (a) the semi-width $a = \pi/m$ (which is independent of $\bar{Q}$) and (b) the maximum thickness $h_{\rm m}$ given by (13)–(15) as functions of the scaled angle α/π for a rivulet of a perfectly wetting fluid with $\beta = \bar{\beta} = 0$ for $\bar{Q} = 0.1, 1, 10, 10^2, 10^3$ when $\lambda = 1$.

in the limit of weak slip, $\lambda \to 0^+$, and becomes shallow according to

$$h_{\mathrm{m}} \sim \left(\frac{4\bar{Q}m}{3\pi\lambda \sin\alpha} \right)^{\frac{1}{2}} \to 0^+ \tag{20}$$

in the limit of strong slip, $\lambda \to \infty$. Figure 5 also illustrates that h_{m} is a monotonically increasing function of $\bar{Q}$, and that the rivulet becomes shallow according to (20) in the limit of small flux, $\bar{Q} \to 0^+$, and becomes deep according to

$$h_{\mathrm{m}} \sim \left(\frac{24\bar{Q}m}{5\pi \sin\alpha} \right)^{\frac{1}{3}} \to \infty \tag{21}$$

in the limit of large flux, $\bar{Q} \to \infty$.

IV. A RIVULET WITH CONSTANT WIDTH $a = \bar{a}\,(> 0)$

Setting $a = \bar{a}$ and $Q = \bar{Q}$ in (7) yields a cubic polynomial equation for β, namely

$$\beta^3 + \frac{9\lambda m g(m\bar{a})}{f(m\bar{a})}\beta^2 - \frac{9\bar{Q}m^4}{f(m\bar{a})\sin\alpha} = 0. \tag{22}$$

In the special case $\lambda = 0$ we recover the solution for $\beta = \beta_0$ and hence for $h_{\mathrm{m}} = h_{\mathrm{m}0} = \beta_0 H(m\bar{a}, 0)/m$ first obtained by Paterson *et al.* [26, Sec. 4], namely

$$\beta_0 = \left(\frac{9\bar{Q}m^4}{f(m\bar{a})\sin\alpha} \right)^{\frac{1}{3}} \quad \text{and} \quad h_{\mathrm{m}0} = \left(\frac{9\bar{Q}m}{f(m\bar{a})\sin\alpha} \right)^{\frac{1}{3}} H(m\bar{a}, 0), \tag{23}$$

while in the general case $\lambda > 0$ the solution for β is

$$\beta = \frac{3\lambda m g(m\bar{a})}{f(m\bar{a})} \left\{ 2\cos\left[\frac{1}{3}\cos^{-1}\left(\frac{\bar{Q}m f(m\bar{a})^2}{6\lambda^3 g(m\bar{a})^3 \sin\alpha} - 1 \right) \right] - 1 \right\} \tag{24}$$

when $0 < \bar{Q}m f(m\bar{a})^2 \leq 12\lambda^3 g(m\bar{a})^3 \sin\alpha$ and

$$\beta = \frac{3\lambda m g(m\bar{a})}{f(m\bar{a})} \left\{ 2\cosh\left[\frac{1}{3}\cosh^{-1}\left(\frac{\bar{Q}m f(m\bar{a})^2}{6\lambda^3 g(m\bar{a})^3 \sin\alpha} - 1 \right) \right] - 1 \right\} \tag{25}$$

when $\bar{Q}m f(m\bar{a})^2 \geq 12\lambda^3 g(m\bar{a})^3 \sin\alpha$, with the corresponding solution for h_{m} given by

$$h_{\mathrm{m}} = \frac{\beta}{m} H(m\bar{a}, 0). \tag{26}$$

Paterson *et al.* [26, Sec. 4] showed in the special case $\lambda = 0$ that the behaviour is qualitatively different for a narrow rivulet with $a = \bar{a} \leq \pi$ and a wide rivulet with $a = \bar{a} > \pi$, and since, as we shall now describe, the same is true in the general case $\lambda > 0$, we treat these two cases separately in what follows.

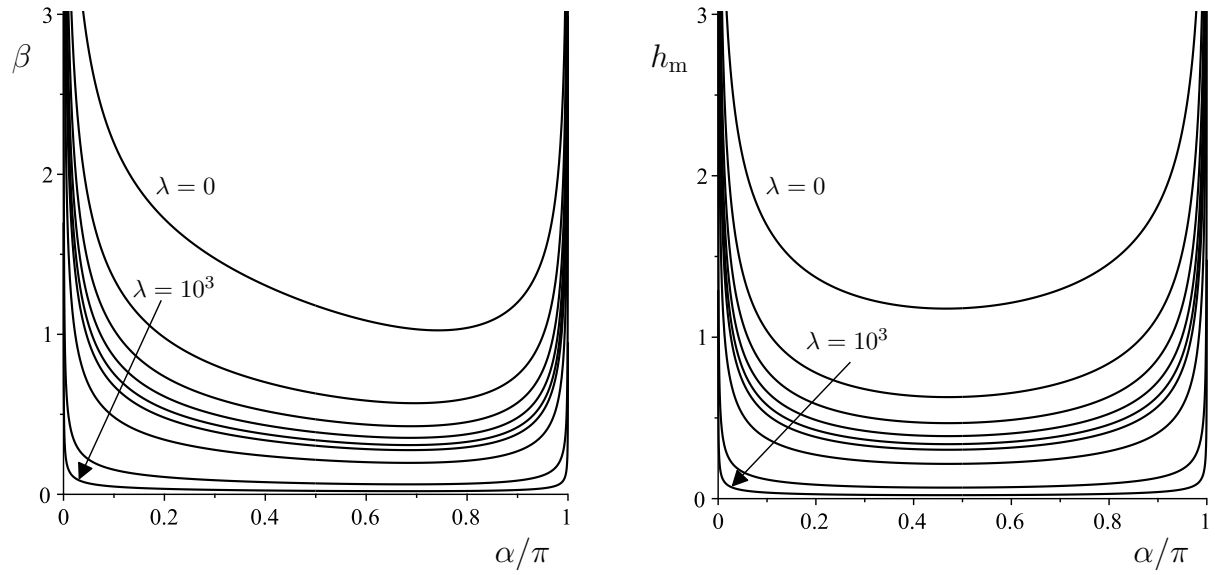

FIG. 6: Plots of (a) the contact angle β and (b) the maximum thickness $h_{\rm m}$ given by (23)–(26) as functions of the scaled angle α/π for a narrow rivulet with constant width $a = \bar{a} = 2\,(< \pi)$ for $\lambda = 0, 1, 2, 3, 4, 5, 10, 10^2, 10^3$ when $\bar{Q} = 1$.

A. A narrow rivulet with $a = \bar{a} \leq \pi$

For a narrow rivulet with $a = \bar{a} \leq \pi$ the solution given by (23)–(26) corresponds to a rivulet that runs all the way from $\alpha = 0$ to $\alpha = \pi$.

Figures 6 and 7 show plots of the contact angle β and the maximum thickness $h_{\rm m}$ given by (23)–(26) plotted as functions of the scaled angle α/π for a narrow rivulet with constant width $a = \bar{a} = 2\,(< \pi)$ for a range of values of λ and $\bar{Q}$, respectively. In particular, Figures 6 and 7 illustrate that (except in the marginal case $\bar{a} = \pi$ in which β is a monotonically decreasing function of α) both β and $h_{\rm m}$ always have single global minima as functions of α, and that the rivulet becomes deep according to

$$\beta \sim \left(\frac{9\bar{Q}}{f(\bar{a})\alpha}\right)^{\frac{1}{3}} \to \infty \quad \text{and} \quad h_{\rm m} \sim \left(\frac{9\bar{Q}}{f(\bar{a})\alpha}\right)^{\frac{1}{3}} \tanh\left(\frac{\bar{a}}{2}\right) \to \infty \tag{27}$$

as $\alpha \to 0^+$, and deep (except in the marginal case $\bar{a} = \pi$ in which $\beta \to 0^+$ and $h_{\rm m} \to \infty$) according to

$$\beta \sim \left(\frac{9\bar{Q}}{f(\bar{a})(\pi - \alpha)}\right)^{\frac{1}{3}} \to \infty \quad \text{and} \quad h_{\rm m} \sim \left(\frac{9\bar{Q}}{f(\bar{a})(\pi - \alpha)}\right)^{\frac{1}{3}} \tan\left(\frac{\bar{a}}{2}\right) \to \infty \tag{28}$$

as $\alpha \to \pi^-$. Figure 6 also illustrates that both β and $h_{\rm m}$ are monotonically decreasing functions of λ, and that the rivulet approaches its finite contact angle and maximum thickness in the case $\lambda = 0$ given by (23) from below

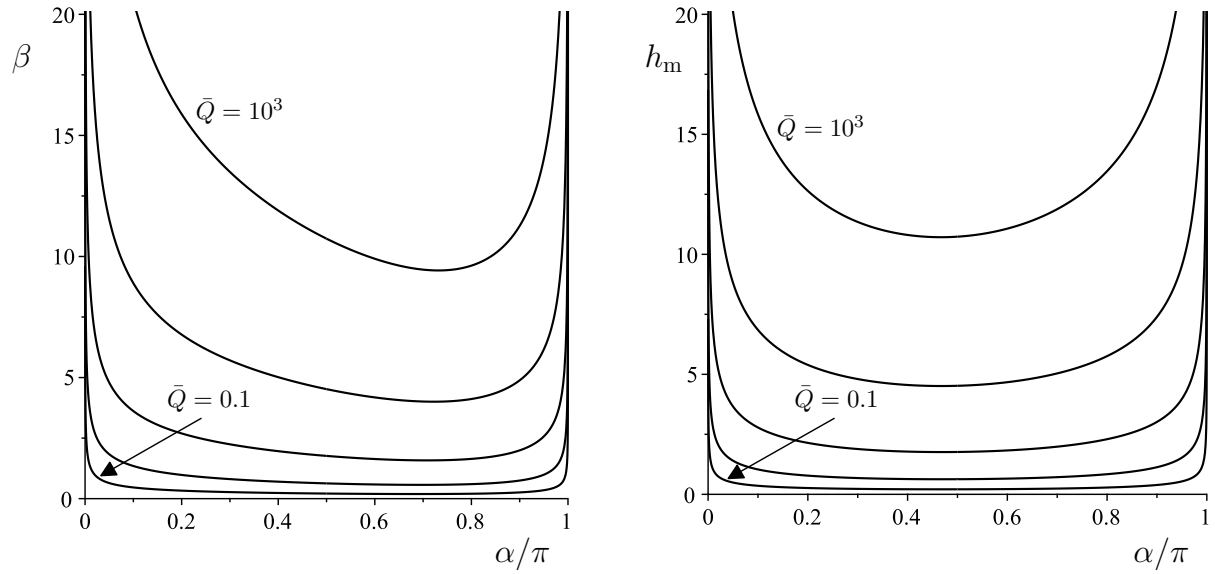

(a) (b)

FIG. 7: Plots of (a) the contact angle β and (b) the maximum thickness $h_{\rm m}$ given by (23)–(26) as functions of the scaled angle α/π for a narrow rivulet with constant width $a = \bar{a} = 2\,(< \pi)$ for $\bar{Q} = 0.1, 1, 10, 10^2, 10^3$ when $\lambda = 1$.

according to

$$\beta = \beta_0 - \frac{3mg(m\bar{a})}{f(m\bar{a})}\lambda + O\left(\lambda^2\right) \to \beta_0^- \quad \text{and} \quad h_{\rm m} = \frac{\beta}{m} H(m\bar{a}, 0) \to h_{\rm m0}^- \tag{29}$$

in the limit of weak slip, $\lambda \to 0^+$, and becomes shallow according to

$$\beta \sim \left(\frac{\bar{Q}m^3}{\lambda g(m\bar{a})\sin\alpha}\right)^{\frac{1}{2}} \to 0^+ \quad \text{and} \quad h_{\rm m} = \left(\frac{\bar{Q}m}{\lambda g(m\bar{a})\sin\alpha}\right)^{\frac{1}{2}} H(m\bar{a}, 0) \to 0^+ \tag{30}$$

in the limit of strong slip, $\lambda \to \infty$. Figure 7 also illustrates that both β and $h_{\rm m}$ are monotonically increasing functions of $\bar{Q}$, and that the rivulet becomes shallow according to (30) in the limit of small flux, $\bar{Q} \to 0^+$, and becomes deep according to

$$\beta \sim \left(\frac{9\bar{Q}m^4}{f(m\bar{a})\sin\alpha}\right)^{\frac{1}{3}} \to \infty \quad \text{and} \quad h_{\rm m} = \left(\frac{9\bar{Q}m}{f(m\bar{a})\sin\alpha}\right)^{\frac{1}{3}} H(m\bar{a}, 0) \to \infty \tag{31}$$

in the limit of large flux, $\bar{Q} \to \infty$. Alshaikhi [32] gives some further details about the minima of β and $h_{\rm m}$ as functions of α.

B. A wide rivulet with $a = \bar{a} > \pi$

For a wide rivulet with $a = \bar{a} > \pi$ the solution given by (23)–(26) corresponds to a rivulet that runs from $\alpha = 0$ to $\alpha = \alpha_{\rm c}$ with monotonically decreasing contact angle β which attains its minimum physically realisable value of zero at $\alpha = \alpha_{\rm c}$, where the critical angle $\alpha_{\rm c} = \alpha_{\rm c}(\bar{a})$ $(\pi/2 < \alpha_{\rm c} < \pi)$ is a monotonically decreasing function of $\bar{a}$ given by

$$\alpha_{\rm c} = \cos^{-1}\left(-\frac{\pi^2}{\bar{a}^2}\right). \tag{32}$$

Note that $\alpha_{\rm c}$ is independent of λ, and so is identical to the corresponding critical angle first identified by Paterson *et al.* [26, Sec. 4.3] in the case $\lambda = 0$. Beyond $\alpha = \alpha_{\rm c}$ the solution given by (23)–(26) predicts that $\beta < 0$ and so is not physically realisable; we therefore follow Paterson *et al.* [26, Sec. 4.3] and assume that the contact lines de-pin at $\alpha = \alpha_{\rm c}$ and that the rivulet runs from $\alpha = \alpha_{\rm c}$ to $\alpha = \pi$ with $\beta \equiv 0$ according to the solution for a rivulet of a perfectly wetting fluid described in Section II A. Note that Paterson *et al.* [26, Sec. 6] also discuss the de-pinning and possible subsequent re-pinning of the contact lines at a positive value of β, but, for simplicity, we restrict our attention to de-pinning at $\beta = 0$ in the present work.

Figures 8 and 9 show plots of the contact angle β given by (23)–(25) for $0 \leq \alpha \leq \alpha_{\rm c}$ and by $\beta \equiv 0$ for $\alpha_{\rm c} \leq \alpha \leq \pi$ and the maximum thickness $h_{\rm m}$ given by (23) and (26) for $0 \leq \alpha \leq \alpha_{\rm c}$ and by (13)–(15) for $\alpha_{\rm c} \leq \alpha \leq \pi$ plotted as functions of the scaled angle α/π for a wide rivulet with constant width $a = \bar{a} = 5\,(> \pi)$ for a range of values of λ and $\bar{Q}$, respectively. The dots denote the values of $\beta = 0$ and $h_{\rm m} = h_{\rm mc}$ at $\alpha = \alpha_{\rm c}$ at which de-pinning occurs. In particular, Figures 8 and 9 illustrate that β is a monotonically decreasing function of α for $0 \leq \alpha \leq \alpha_{\rm c}$ and $h_{\rm m}$ always has a single global minimum as a function of α, and that the rivulet becomes deep according to (27) as $\alpha \to 0^+$, and deep with finite semi-width $a = \pi$ according to (17) and (18) as $\alpha \to \pi^-$. Figures 8 and 9 also illustrate that both β and $h_{\rm m}$ are monotonically decreasing functions of λ and monotonically increasing functions of $\bar{Q}$, and behave in the same manner as that described in Section IV A for $0 \leq \alpha \leq \alpha_{\rm c}$ and in Section III for $\alpha_{\rm c} \leq \alpha \leq \pi$. In addition, Figures 8 and 9 also illustrate that $\beta = O(\alpha_{\rm c} - \alpha) \to 0^+$ as $\alpha \to \alpha_{\rm c}^-$ and $h_{\rm m} = h_{\rm mc} + O(\alpha_{\rm c} - \alpha) \to h_{\rm mc}$ as $\alpha \to \alpha_{\rm c}$. Alshaikhi [32] gives some further details about the minima of β and $h_{\rm m}$ as functions of α.

V. A RIVULET WITH POSITIVE CONSTANT CONTACT ANGLE $\beta = \bar{\beta}\,(> 0)$

The solution for a rivulet with constant contact angle $\beta = \bar{\beta}$ in the special case of a perfectly wetting fluid with zero contact angle, $\bar{\beta} = 0$, has already been described in Section III, and so in this Section we consider the solution

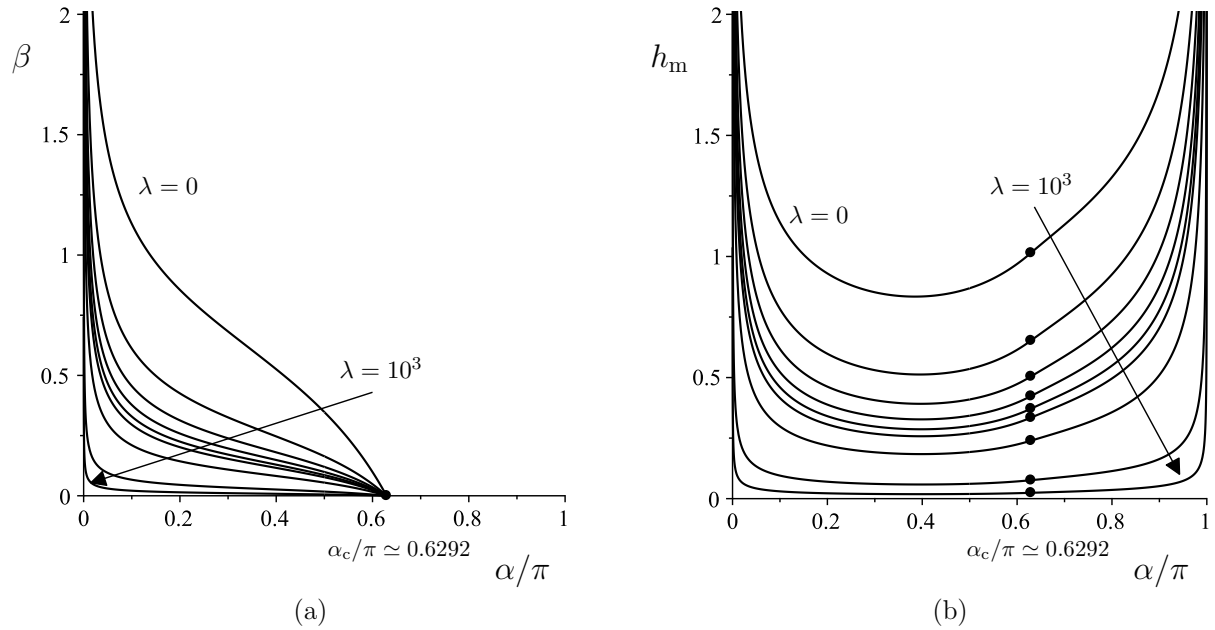

FIG. 8: Plots of (a) the contact angle β given by (23)–(25) for $0 \leq \alpha/\pi \leq \alpha_{\rm c}/\pi \simeq 0.6292$ and by $\beta \equiv 0$ for $\alpha_{\rm c}/\pi \leq \alpha/\pi \leq 1$ and (b) the maximum thickness $h_{\rm m}$ given by (23) and (26) for $0 \leq \alpha/\pi \leq \alpha_{\rm c}/\pi$ and by (13)–(15) for $\alpha_{\rm c}/\pi \leq \alpha/\pi \leq 1$ as functions of the scaled angle α/π for a wide rivulet with constant width $a = \bar{a} = 5\,(> \pi)$ for $\lambda = 0, 1, 2, 3, 4, 5, 10, 10^2, 10^3$ when $\bar{Q} = 1$. The dots ($\bullet$) denote the values of $\beta = 0$ and $h_{\rm m} = h_{\rm mc}$ at $\alpha = \alpha_{\rm c}$ at which de-pinning occurs.

in the general case of a non-perfectly wetting fluid with positive constant contact angle, $\bar{\beta} > 0$.

Setting $\beta = \bar{\beta}\,(> 0)$ and $Q = \bar{Q}$ in (7) yields a transcendental equation for a, namely

$$f(ma) + \frac{9\lambda m}{\bar{\beta}}\, g(ma) - \frac{9\bar{Q}m^4}{\bar{\beta}^3 \sin\alpha} = 0. \tag{33}$$

Even in the special case $\lambda = 0$ the solution of (33) cannot, in general, be obtained analytically, but may readily be obtained numerically as well as analytically in various asymptotic limits, and corresponds to a rivulet that runs all the way from $\alpha = 0$ to $\alpha = \pi$. In the special case $\lambda = 0$ we recover the solution for $a = a_0$ and hence for $h_{\rm m} = h_{\rm m0} = \bar{\beta} H(ma_0, 0)/m$ first obtained by Duffy and Moffatt [27] (see also, for example, Paterson *et al.* [26, Sec. 3]).

Figures 10 and 11 show plots of the semi-width a obtained by solving (33) and the maximum thickness $h_{\rm m}$ given by (7) plotted as functions of the scaled angle α/π for a rivulet with constant contact angle $\beta = \bar{\beta} = 1$ for a range of values of λ and $\bar{Q}$, respectively. In particular, Figures 10 and 11 illustrate that a always has and $h_{\rm m}$ may or may not have single global minima as functions of α, and that the rivulet becomes wide with finite maximum thickness

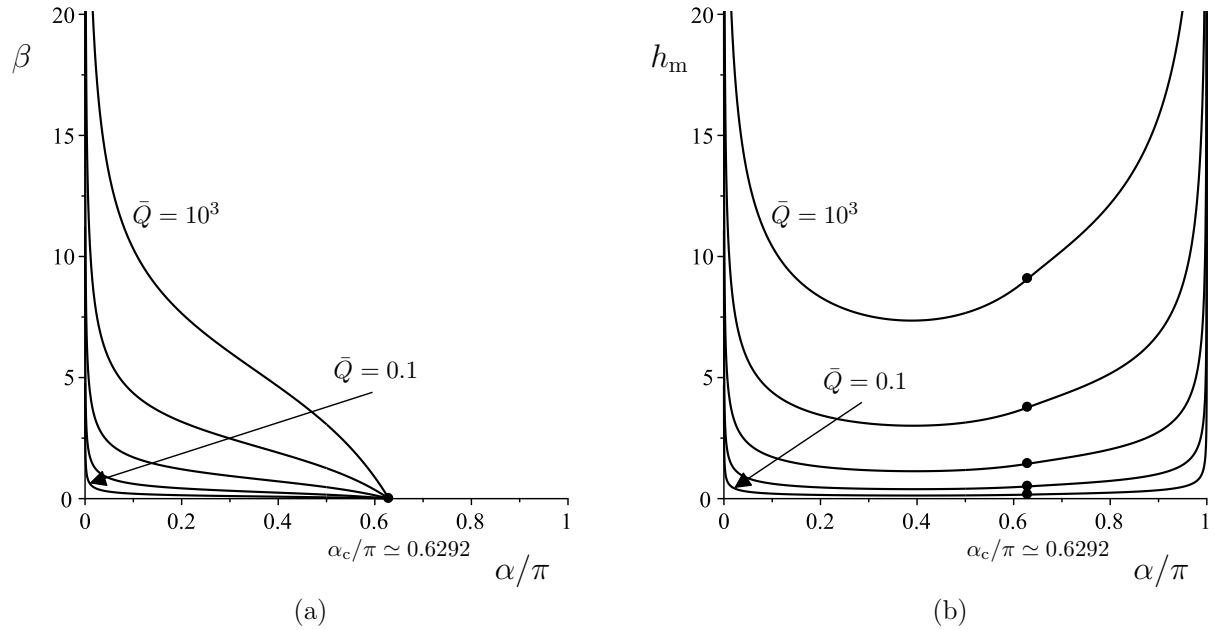

FIG. 9: Plots of (a) the contact angle β given by (23)–(25) for $0 \le \alpha/\pi \le \alpha_c/\pi \simeq 0.6292$ and by $\beta \equiv 0$ for $\alpha_c/\pi \le \alpha/\pi \le 1$ and (b) the maximum thickness h_m given by (23) and (26) for $0 \le \alpha/\pi \le \alpha_c/\pi$ and by (13)–(15) for $\alpha_c/\pi \le \alpha/\pi \le 1$ as functions of the scaled angle α/π for a wide rivulet with constant width $a = \bar{a} = 5\,(> \pi)$ for $\bar{Q} = 0.1, 1, 10, 10^2, 10^3$ when $\lambda = 1$. The dots ($\bullet$) denote the values of $\beta = 0$ and $h_m = h_{mc}$ at $\alpha = \alpha_c$ at which de-pinning occurs.

$h_m = \bar{\beta}$ according to

$$a \sim \frac{3\bar{Q}}{2\bar{\beta}^2(\bar{\beta} + 3\lambda)\alpha} \to \infty \quad \text{and} \quad h_m = \bar{\beta} + \frac{\bar{\beta}}{4}\alpha^2 + O\left(\alpha^4\right) \to \bar{\beta}^+ \tag{34}$$

as $\alpha \to 0^+$, and deep with finite semi-width $a = \pi$ according to

$$a = \pi - \left(\frac{5\pi\bar{\beta}^3(\pi - \alpha)}{3\bar{Q}}\right)^{\frac{1}{3}} + O\left((\pi - \alpha)^{\frac{2}{3}}\right) \to \pi^- \tag{35}$$

and

$$h_m = \left(\frac{24\bar{Q}}{5\pi(\pi - \alpha)}\right)^{\frac{1}{3}} - \frac{6\lambda}{5} + O\left((\pi - \alpha)^{\frac{1}{3}}\right) \to \infty \tag{36}$$

as $\alpha \to \pi^-$. Figure 10 also illustrates that both a and h_m are monotonically decreasing functions of λ, and that the rivulet approaches its finite semi-width and maximum thickness in the case $\lambda = 0$ from below according to

$$a = a_0 - \frac{9g(ma_0)}{\bar{\beta}f'(ma_0)}\lambda + O\left(\lambda^2\right) \to a_0^- \quad \text{and} \quad h_m = \frac{\bar{\beta}}{m}H(ma_0, 0) \to h_{m0}^- \tag{37}$$

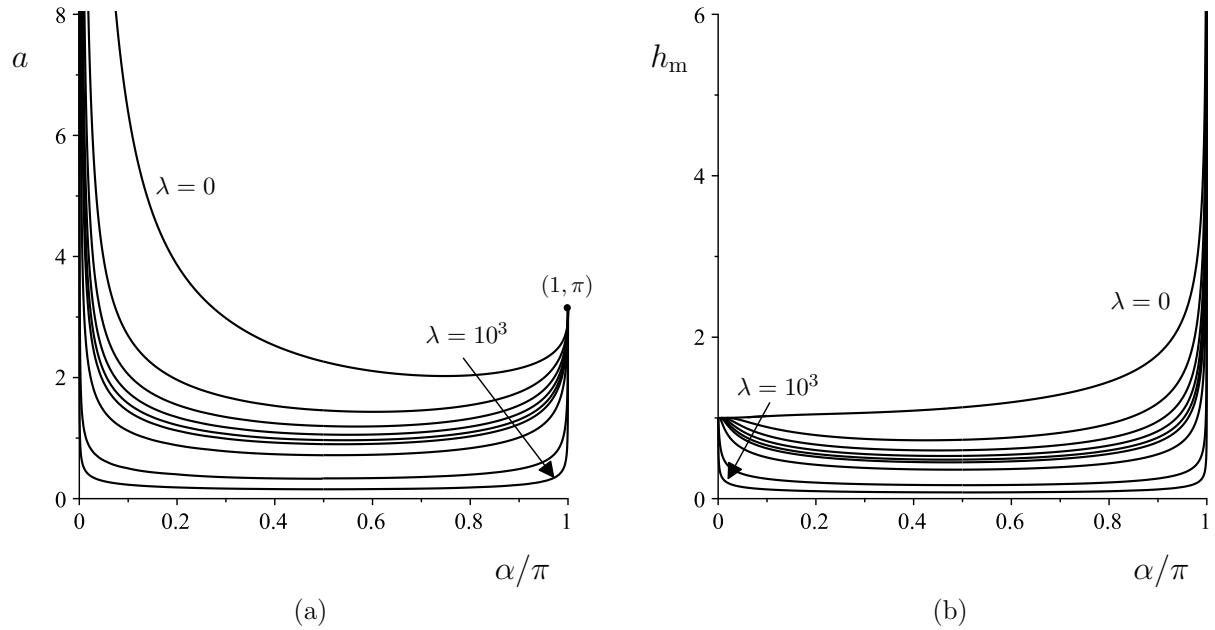

FIG. 10: Plots of (a) the semi-width a obtained by solving (33) and (b) the maximum thickness $h_{\rm m}$ given by (7) as functions of the scaled angle α/π for a rivulet with constant contact angle $\beta = \bar{\beta} = 1$ for $\lambda = 0, 1, 2, 3, 4, 5, 10, 10^2, 10^3$ when $\bar{Q} = 1$.

in the limit of weak slip, $\lambda \to 0^+$, and becomes narrow and shallow according to

$$a \sim \left(\frac{15\bar{Q}}{4\bar{\beta}^2\lambda\sin\alpha}\right)^{\frac{1}{3}} \to 0^+ \quad \text{and} \quad h_{\rm m} \sim \left(\frac{15\bar{\beta}\bar{Q}}{32\lambda\sin\alpha}\right)^{\frac{1}{3}} \to 0^+ \tag{38}$$

in the limit of strong slip, $\lambda \to \infty$. Figure 11 also illustrates that both a and $h_{\rm m}$ are monotonically increasing functions of $\bar{Q}$, and that the rivulet becomes narrow and shallow according to (38) in the limit of small flux, $\bar{Q} \to 0^+$, and becomes wide with finite maximum thickness $h_{\rm m} = \bar{\beta}/m$ from below according to

$$a \sim \frac{3\bar{Q}m^3}{2\bar{\beta}^2(\bar{\beta} + 3\lambda m)\sin\alpha} \to \infty \tag{39}$$

and

$$h_{\rm m} \sim \frac{\bar{\beta}}{m}\tanh\left(\frac{3\bar{Q}m^4}{4\bar{\beta}^2(\bar{\beta} + 3\lambda m)\sin\alpha}\right) \to \frac{\bar{\beta}}{m}^- \tag{40}$$

for $0 \le \alpha < \pi/2$, wide and deep according to

$$a = \left(\frac{105\bar{Q}}{4\bar{\beta}^3}\right)^{\frac{1}{4}} - \frac{7\lambda}{4\bar{\beta}} + O\left(\frac{1}{\bar{Q}^{\frac{1}{4}}}\right) \to \infty \tag{41}$$

and

$$h_{\rm m} = \left(\frac{105\bar{\beta}\bar{Q}}{64}\right)^{\frac{1}{4}} - \frac{7\lambda}{8} + O\left(\frac{1}{\bar{Q}^{\frac{1}{4}}}\right) \to \infty \tag{42}$$

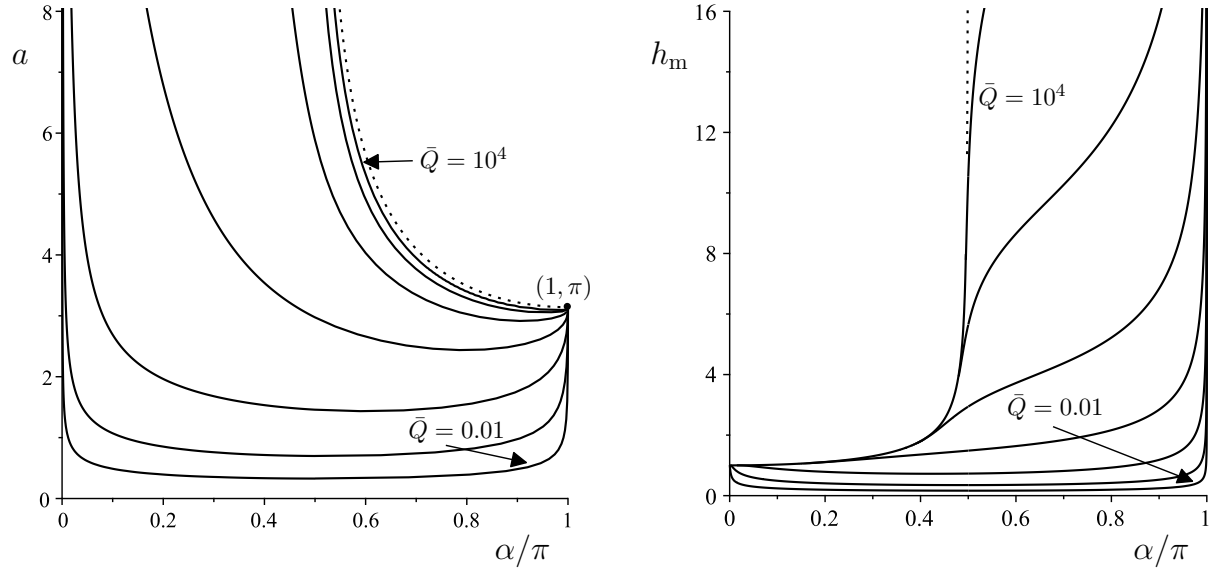

(a) (b)

FIG. 11: Plots of (a) the semi-width a obtained by solving (33) and (b) the maximum thickness $h_{\rm m}$ given by (7) as functions of the scaled angle α/π for a rivulet with constant contact angle $\beta = \bar{\beta} = 1$ for $\bar{Q} = 0.01, 0.1, 1, 10, 10^2, 10^3, 10^4$ when $\lambda = 1$. The dotted lines denote the leading order solutions in the limit $\bar{Q} \to \infty$ given by $a = \pi/m$ for $\pi/2 < \alpha \leq \pi$ in (a) and by $h_{\rm m} = \bar{\beta}/m$ for $0 \leq \alpha < \pi/2$ in (b).

at $\alpha = \pi/2$, and deep with finite semi-width $a = \pi/m$ from below according to

$$a = \frac{\pi}{m} - \frac{1}{m^2}\left(\frac{5\pi\bar{\beta}^3 \sin\alpha}{3\bar{Q}m}\right)^{\frac{1}{3}} + O\left(\frac{1}{\bar{Q}^{\frac{2}{3}}}\right) \to \frac{\pi}{m}^{-} \tag{43}$$

and

$$h_{\rm m} \sim \left(\frac{24\bar{Q}m}{5\pi \sin\alpha}\right)^{\frac{1}{3}} \to \infty \tag{44}$$

for $\pi/2 < \alpha \leq \pi$, in the limit of large flux, $\bar{Q} \to \infty$. Alshaikhi [32] gives some further details about the minima of a and $h_{\rm m}$ as functions of α.

VI. CONCLUSIONS

Motivated by our interest in the behaviour of a fluid at the surface of a porous medium and at a superhydrophobic textured surface impregnated with either gas or a lubricant, as well as in microfluidics with fluid walls, in the present work we undertook a detailed analysis of small-scale locally unidirectional gravity-driven rivulet flow with prescribed

volume flux down an inclined slippery substrate for a rivulet with either constant width (*i.e.*, pinned contact lines) $a = \bar{a}$ or constant contact angle $\beta = \bar{\beta}$. In particular, we determined the effect that varying the slip length λ (*i.e.*, the strength of the slip at the solid–fluid interface) has on the rivulet. The present analysis shows that, while many of the qualitative features of the rivulet (such as, for example, that a rivulet of perfectly wetting fluid is possible only for $\pi/2 < \alpha \leq \pi$, and that a rivulet with constant width is possible only if either the rivulet is narrow, or for $0 \leq \alpha \leq \alpha_{\rm c}$, where $\alpha_{\rm c}$ is given by (32), if the rivulet is wide) are the same as in the classical case of no slip, $\lambda = 0$, the shape and size of the rivulet and the velocity within it depend strongly on the value of λ. Increasing the value of λ reduces the viscous resistance at the substrate and hence leads to a larger velocity within the rivulet, and so the prescribed flux is achieved with a smaller rivulet. In particular, in the limit of strong slip, $\lambda \to \infty$, for a rivulet of a perfectly wetting fluid and a rivulet with constant width the velocity becomes large and plug-like like $O(\lambda^{1/2}) \gg 1$ and the rivulet becomes shallow like $O(\lambda^{-1/2}) \ll 1$, while for a rivulet with positive constant contact angle the velocity becomes large and plug-like like $O(\lambda^{2/3}) \gg 1$ and the rivulet becomes narrow like $O(\lambda^{-1/3}) \ll 1$ and shallow like $O(\lambda^{-1/3}) \ll 1$.

The present analysis employed the simplest and most widely used slip condition, namely the Navier slip condition given by (1), but we do not anticipate that using other slip conditions would lead to significant qualitative changes in the behaviour of the rivulet. For example, the stronger Greenspan slip condition introduced by Greenspan [33] (and used, for example, by Wilson, Hunt and Duffy [34]) replaces the constant Navier slip length λ with the non-constant Greenspan slip length $\lambda_{\rm G}/h$, so that the velocity (2) and the local flux (3) become

$$u = \frac{\sin\alpha}{2}\left[2(hz + \lambda_{\rm G}) - z^2\right] \quad \text{and} \quad \bar{u} = \frac{\sin\alpha}{3}h(h^2 + 3\lambda_{\rm G}), \tag{45}$$

respectively, and hence the volume fluxes in (6) and (7) become

$$Q = \frac{\pi\sin\alpha}{24m}h_{\rm m}(5h_{\rm m}^2 + 24\lambda_{\rm G}) \quad \text{and} \quad Q = \frac{\beta^3\sin\alpha}{9m^4}f(ma) + \frac{\lambda_{\rm G}\beta\sin\alpha}{m^2}g_{\rm G}(ma), \tag{46}$$

respectively, where the function $g_{\rm G}(ma)$ is given by

$$g_{\rm G}(ma) = \begin{cases} 2(ma\coth ma - 1) & \text{for} \quad 0 \leq \alpha < \dfrac{\pi}{2}, \\ \dfrac{2}{3}(ma)^2 & \text{for} \quad \alpha = \dfrac{\pi}{2}, \\ 2(1 - ma\cot ma) & \text{for} \quad \dfrac{\pi}{2} < \alpha \leq \pi, \end{cases} \tag{47}$$

which can be analysed in the same way as we have done in the present work for Navier slip. In particular, in the limit of strong Greenspan slip, $\lambda_{\rm G} \to \infty$, the behaviour of the rivulet is qualitatively similar to that in the limit of strong Navier slip, $\lambda \to \infty$, described above with $O(\lambda^{1/2})$ and $O(\lambda^{-1/2})$ replaced by $O(\lambda_{\rm G})$ and $O({\lambda_{\rm G}}^{-1})$, respectively, for

a rivulet of a perfectly wetting fluid and a rivulet with constant width, and with $O(\lambda^{2/3})$ and $O(\lambda^{-1/3})$ replaced by $O(\lambda_{\mathrm{G}})$ and $O({\lambda_{\mathrm{G}}}^{-1/2})$, respectively, for a rivulet with positive constant contact angle.

ACKNOWLEDGEMENTS

All three of the authors wish to thank Dr Michael Grinfeld (University of Strathclyde) for his many insightful contributions during the course of the present work. The first author (ASA) wishes to thank the Ministry of Education, Kingdom of Saudi Arabia and King Abdulaziz University for their financial support of his PhD research at the University of Strathclyde in Glasgow.

DATA AVAILABILITY STATEMENT

The data that supports the findings of this study are available within the article.

[1] A. A. Darhuber and S. M. Troian, "Principles of microfluidic actuation by modulation of shear stresses", *Annu. Rev. Fluid Mech.* **37** 425–455 (2005)

[2] R. W. Griffiths, "The dynamics of lava flows", *Annu. Rev. Fluid Mech.* **32** 477–518 (2000)

[3] S. V. Alekseenko, S. P. Aktershev, A. V. Bobylev, S. M. Kharlamov, and D. M. Markovich, "Nonlinear forced waves in a vertical rivulet flow", *J. Fluid Mech.* **770** 350–373 (2015)

[4] M. A. Herrada, A. S. Mohamed, J. M. Montanero, and A. M. Gañán-Calvo, "Stability of a rivulet flowing in a microchannel", *Int. J. Multiphase Flow* **69** 1–7 (2015)

[5] K. Mahady, S. Afkhami, and L. Kondic, "On the influence of initial geometry on the evolution of fluid filaments", *Phys. Fluids* **27** 092104 (2015)

[6] P. D. Howell, H. Kim, M. G. Popova, and H. A. Stone, "Rivulet flow over a flexible beam", *J. Fluid Mech.* **796** 285–305 (2016)

[7] F. H. H. Al Mukahal, B. R. Duffy, and S. K. Wilson, "Advection and Taylor–Aris dispersion in rivulet flow", *Proc. Roy. Soc. A* **473** 20170524 (2017)

[8] F. H. H. Al Mukahal, B. R. Duffy, and S. K. Wilson, "Rivulet flow of generalized Newtonian fluids", *Phys. Rev. Fluids* **3** 083302 (2018)

[9] E. Lauga, M. P. Brenner, and H. A. Stone, "Microfluidics: the no-slip boundary condition", Chapter 19 in Springer Handbook of Experimental Fluid Mechanics, C. Tropea, A. L. Yarin, J. F. Foss (Eds.), Springer-Verlag Berlin Heidelberg (2007). pp. 1219–1240.

[10] M. Rauscher and S. Dietrich, "Wetting phenomena in nanofluidics", *Annu. Rev. Mater. Res.* **38** 143–172 (2008)

[11] J. P. Rothstein, "Slip on superhydrophobic surfaces", *Annu. Rev. Fluid Mech.* **42** 89–109 (2010)

[12] T. Sochi, "Slip at fluid–solid interface", *Poly. Rev.* **51** 309–340 (2011)

[13] T. Lee, E. Charrault, and C. Neto, "Interfacial slip on rough, patterned and soft surfaces: a review of experiments and simulations", *Adv. Coll. Int. Sci.* **210** 21–38 (2014)

[14] J. M. P. Nicholson, H. Power, O. Tammisola, S. Hibberd, and E. D. Kay, "Fluid dynamics of the slip boundary condition for isothermal rimming flow with moderate inertial effects", *Phys. Fluids* **31** 033602 (2019)

[15] G. S. Beavers and D. D. Joseph, "Boundary conditions at a naturally permeable wall", *J. Fluid Mech.* **30** 197–207 (1967)

[16] W. Jäger and A. Mikelić, "On the interface boundary condition of Beavers, Joseph, and Saffman", *SIAM J. Appl. Math.* **60** 1111–1127 (2000)

[17] M. Le Bars and M. G. Worster, "Interfacial conditions between a pure fluid and a porous medium: implications for binary alloy solidification", *J. Fluid Mech.* **550** 149–173 (2006)

[18] D. A. Nield, "The Beavers–Joseph boundary condition and related matters: a historical and critical note", *Transp. Porous Med.* **78** 537–540 (2009)

[19] D. G. Crowdy, "Slip length for transverse shear flow over a periodic array of weakly curved menisci", *Phys. Fluids* **29** 091702 (2017)

[20] D. G. Crowdy, "Perturbation analysis of subphase gas and meniscus curvature effects for longitudinal flows over superhydrophobic surfaces", *J. Fluid Mech.* **822** 307–326 (2017)

[21] O. Schnitzer and E. Yariv, "Longitudinal pressure-driven flows between superhydrophobic grooved surfaces: large effective slip in the narrow-channel limit", *Phys. Rev. Fluids* **2** 072101(R) (2017)

[22] E. Alinovi and A. Bottaro, "Apparent slip and drag reduction for the flow over superhydrophobic and lubricant-impregnated surfaces", *Phys. Rev. Fluids* **3** 124002 (2018)

[23] E. S. Asmolov, T. V. Nizkaya, and O. I. Vinogradova, "Enhanced slip properties of lubricant-infused grooves", *Phys. Rev. E* **98** 033103 (2018)

[24] E. J. Walsh, A. Feuerborn, J. H. R. Wheeler, A. N. Tan, W. M. Durham, K. R. Foster, and P. R. Cook, "Microfluidics with fluid walls", *Nat. Commun.* **8** 816 (2017)

[25] L. M. Hocking, "The spreading of a thin drop by gravity and capillarity", *Q. J. Mech. Appl. Math.* **36** 55–69 (1983)

[26] C. Paterson, S. K. Wilson, and B. R. Duffy, "Pinning, de-pinning and re-pinning of a slowly varying rivulet", *Euro. J. Mech. B/Fluids* **41** 94–108 (2013)

[27] B. R. Duffy and H. K. Moffatt, "Flow of a viscous trickle on a slowly varying incline", *Chem. Eng. J.* **60** 141–146 (1995)

[28] J. M. Sullivan, S. K. Wilson, and B. R. Duffy, "A thin rivulet of perfectly wetting fluid subject to a longitudinal surface shear stress", *Q. J. Mech. Appl. Math.* **61** 25–61 (2008)

[29] S. K. Wilson and B. R. Duffy, "A rivulet of perfectly wetting fluid draining steadily down a slowly varying substrate", *IMA J. Appl. Math.* **70** 293–322 (2005)

[30] S. K. Wilson, J. M. Sullivan, and B. R. Duffy, "The energetics of the breakup of a sheet and of a rivulet on a vertical substrate in the presence of a uniform surface shear stress", *J. Fluid Mech.* **674** 281–306 (2011)

[31] C. Paterson, S. K. Wilson, and B. R. Duffy, "Rivulet flow round a horizontal cylinder subject to a uniform surface shear stress", *Q. J. Mech. Appl. Math.* **67** 567–597 (2014)

[32] A. S. Alshaikhi, Theoretical Analysis of Some Thin-Film Flows over Complex Surfaces, PhD Thesis, University of Strathclyde, Glasgow (2020)

[33] H. P. Greenspan, "On the motion of a small viscous droplet that wets a surface", *J. Fluid Mech.* **84** 125–143 (1978)

[34] S. K. Wilson, R. Hunt, and B. R. Duffy, "The rate of spreading in spin coating", *J. Fluid Mech.* **413** 65–88 (2000)